THESIS

SECONDARY EMISSION EFFECTS IN ION BEAMS

Submitted by

Carlos A. Marazzi

In partial fulfillment of the requirements

for the Degree of Master of Science

Colorado State University

Fort Collins, Colorado

November, 1964

THESIS

SECONDARY EMISSION EFFECTS IN ION BEAMS

Submitted by

Carlos A. Marazzi

In partial fulfillment of the requirements

for the Degree of Master of Science

Colorado State University

Fort Collins, Colorado

November, 1964

ABSTRACT OF THESIS

SECONDARY EMISSION EFFECTS IN ION BEAMS

17749

There are many reasons to believe that electric propulsion is the most suitable way, known at the present time, of thrusting rockets for very long trips in space. In the last few years, many research works have been conducted on the explanation of phenomena occuring in, and the design of, electrostatic thrustors.

In one of these research works, it was found that the power of an ion-beam engine, when an electron source is introduced into it, increases remarkably in regard to the expected values. This could have been due to a meaningful space charge compensation of the ion beam by secondary emission. This research work attempts to verify this explanation of the phenomenon.

This thesis is based on existing publications that deal with the solution of ambipolar space-charge problems.

The result of the analytical treatment of the proposed model shows that the unexpected power increase could have hardly been due solely to the space-charge compensation.

Carlos Marazzi
Electrical Engineering Department
Colorado State University
November, 1964

ACKNOWLEDGEMENTS

The author wishes to express his appreciation to Professors Virgil A. Sandborn and R. John Morgan for their helpful guidance and counseling.

Sincere thanks are due to Drs. Lee M. Maxwell and Lionel V. Baldwin for their help in discussing various problems associated with this work.

This research was made possible by a grant of the National Aerospace Administration.

TABLE OF CONTENTS

LIST OF FIGURES

INTRODUCTION

Sandborn and Baldwin [1][1] found (during experimentations with a focused ion-beam-thrustor) that the ion-beam-power increases remarkably by introducing, close to the ion-emitter, an electron-source. This increase in beam power is many times over the expected values.

The first part of this thesis gives an outline of thoughts developed during preliminary study of a possible model which might explain the increase of power in the ion-beam-thrustor.

The second part deals with the analytical solution of a proposed model and the evaluation of special cases. The evaluation, using a digital computer, of the potential distribution between infinite parallel plates with space-charges and space-charge-free zones is given in an appendix.

BACKGROUND OF THE PROBLEM

An exact mathematical description of the current increase when two different "charge carriers" are flowing in the same space and in opposite directions is given in Ref. [2] and [3]. Paper [2] by I. Langmuir from the year 1929 describes: electric field, potential, and space-charge distributions.

---

[1] For bracketed references, see Annotated Bibliography on page 18.

LIST OF TABLES

Müller-Lübeck [3] makes a rigorously mathematical analysis using the same model as I. Langmuir. Both consider the ideal case of parallel plane surfaces for the electrodes and zero initial velocity of the "charge carriers". The electric field is zero at the surfaces. These works and others on the subject have concluded that current density increases of about 1.86 times, with respect to the case of the unipolar flow are possible. This density increase occurs when:

$$\frac{J_p}{J_e}\sqrt{\frac{m_p}{m_e}} = 1.0$$

where:

m_p and m_e are the masses of the ions and electrons;

J_p and J_e are the current densities;

that is, when both space charges are of equal number. However, the observed increase of current in the ion-beam-thrustor [1], was up to 25 times greater than without the electron source.

In this case [1], the electron-source was a thoriated tungsten wire ring of 1.43 cm (0.57 inch) diameter heated to about 1370°K. The accelerating potentials used during the experimentation were from 2 to 5 kV, and the focusing used was a Pierce accelerator system. This focusing system assumes a very thin beam, so that in the aperture of the accelerator the potential surface should approximate a plane. In the case of the thrustor, the aperture was 2.05 cm (0.83 inch), and the ratios $\frac{L}{D}$ (D stands for the diameter of the beam

and L for the distance between the accelerators) that were used, were between 0.6 and 1.4. These low values for $\frac{L}{D}$ cause the beam to spread, so that the potential surface in the accelerator's aperture is no longer a plane, and as a consequence the electric field is non-homogeneous. In [1] (Fig. 13 and 14) the amount of power lost by the non-homogeneity is shown.

THE MECHANISM OF THE PHENOMENA

There are various theories with respect to this phenomenon. One possible mechanism is that the electrons arriving to the ion-emitter with high energy produce a large number of secondary electrons. These secondary electrons should create a negative-space charge in the same place or near the ion's "virtual cathode". The potential and the field distributions will be modified, thus reducing the space charge and a greater number of ions can leave the ion's virtual cathode.

In the case here considered the bipolar space charge is created by two sources. One is an ion-emitter in an accelerating field. The other is the secondary emission of electrons produced by primary electrons with high energy coming from an electron-emitter.

SPACE CHARGE DISTRIBUTION IN THE CASE TO BE CONSIDERED

Figure 1 shows the system composed of an ion-emitter and an electron-emitter. The ions are emitted with an initial velocity

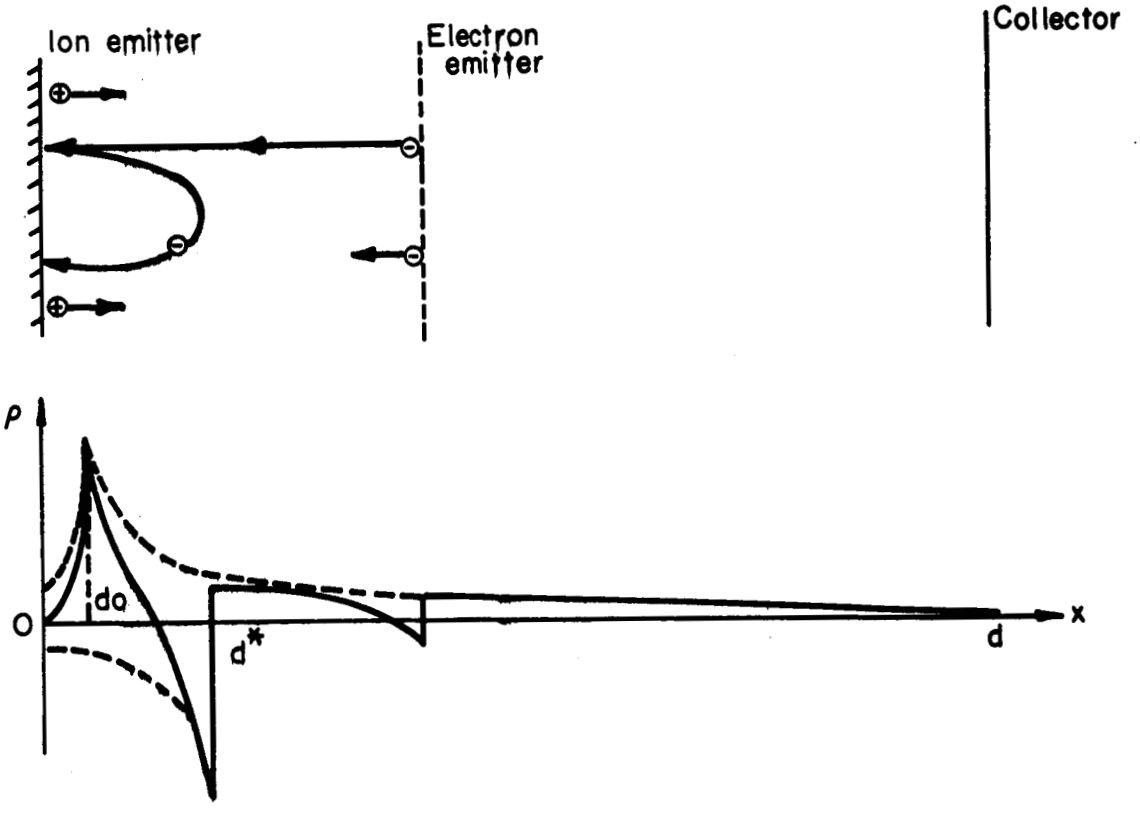

FIG. 1 PROPOSED MODEL WITH AN ION-EMITTER AND AN ELECTRON - EMITTER

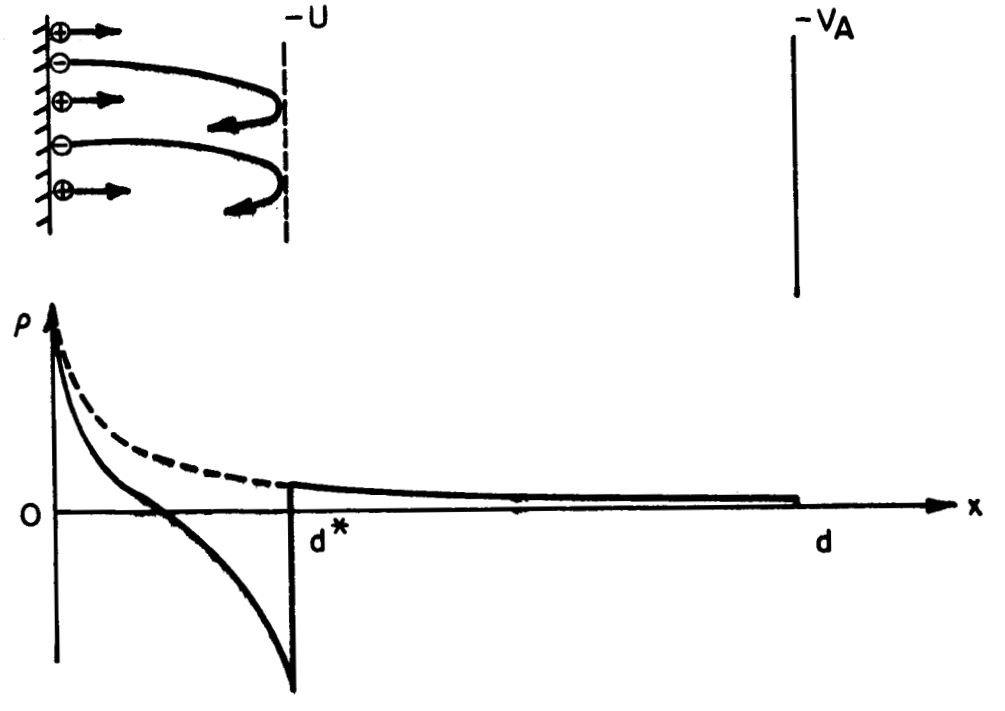

FIG. 2 SIMPLIFIED MODEL

$V_{po} \neq o$ and create in the neighborhood of the emitter a cloud of positive charges. In this cloud the ions have zero uniform velocity and therefore the space charge has a maximum value.

The electrons are emitted also with an initial velocity $V_{eo} \neq o$ and are accelerated in a high potential field, making a very small contribution to the space charge near the ion-emitter.

The electrons arriving at the ion-emitter with high energy produce secondary electrons with energies between 2 to 20 volts. These secondary electrons are in a retarding field and after losing their kinetic energy fall back to the ion-emitter and probably cause tertiary electrons. In this way a negative space charge is created near the emitter which reduces the space charge-limitation of the ions. Figure 1 shows also the approximate space charge distribution.

To study the problem of the ion current increase due to the effect of the negative space-charges only the space between d_o and d^* is considered. This is done because the space between $x = o$ and $x = d_o$ is influenced mainly by the ions space charge, where the ions have velocities between the thermal initial velocity V_{po} and zero at d_o. The space between d^* and d is mainly influenced by the accelerating ions and the secondary electrons. Because the primary electron source will give a secondary contribution only and may not be parallel to the ion beam, it is not considered in the study of ion current increase. The result of these simplifications is the model

shown in Figure 2. The secondary electron-space charge has a finite value at the surface of the emitter given by the initial velocities of the electrons, and it increases in almost hyperbolic form until the point d*. At d* the electrons lose their kinetic energy and the space charge reaches a maximum. Therefore, with regard to the space charge effects, the electron current going from the emitter to d*, and the one coming back to the emitter, can be considered as twice the current flowing from d* to the emitter. The electrons have zero initial velocity at d* and a finite velocity V_{eo} at the emitter.

For the space between x = o and x = d*, the problem is similar to the one explained in [2] and [3]. The main differences are: the distance between "plates" is not constant and a decrease of the distance can give a further increase of the current; and the ratio of space charges is a function of the primary electron current, which can be controlled by the temperature of the electron emitter.

The location where the electrons have zero velocity and turn back to the emitter will always be beyond the main positive space charge region, because as long as the electrons are moving in the positive space charge they do not see a meaningful retarding potential. There is no possibility that the maximum of the negative charge can be at the same location as the positive charge. However, there must be a location where the negative space charge has a maximum, because there is a location where the electrons have zero velocity and

fall back to the emitter. Thus a partial "neutralization" of the positive space charge takes place.

Assuming the absence of electrons and zero initial velocity for the ions, the ion current density [5] is given by

$$J_{po} = \frac{4}{9} \epsilon_o \sqrt{\frac{2e}{m_p}} \frac{V_A^{3/2}}{d^2} \tag{1}$$

where J_{po} = ion current density in A/cm^2;

d = distance between emitter and point where the potential is V_A;

e = charge of each ion. (It is considered of the same absolute value as the charge of an electron, because it is assumed that there is single ionization only.)

POISSON'S EQUATION FOR TWO DIFFERENT SPACE CHARGES FLOWING IN THE SAME DIRECTION

To find the ion current increase due to presence of secondary electrons at the ion-emitter's surface, we solve the Poisson's equation for the simplified model explained above.

Here we make use again of Figure 2. In this case the ions are in an accelerating field and the electrons in a retarding field. Thus the energy equations are

$$\frac{1}{2} m_p v_p^2 = eV \tag{2}$$

$$\frac{1}{2} m_e v_e^2 = \frac{1}{2} m_e v_{eo}^2 - eV \tag{3}$$

which gives $$v_p = \sqrt{\frac{2e}{m_p}}\ \sqrt{V} \tag{4}$$

and $$v_e = \sqrt{v_{eo}^2 - \frac{2e}{m_e}\ V} \tag{5}$$

The general expression of Poisson's equation is:

$$\frac{d^2V}{dx^2} + \frac{1}{\epsilon_o}\sum \rho = 0 \tag{6}$$

$$\sum \rho = \rho_p - \rho_e \tag{7}$$

$$\frac{d^2V}{dx^2} = \frac{1}{\epsilon_o}\ (\rho_e - \rho_p) \tag{8}$$

and in terms of the current densities and velocities

$$\frac{d^2V}{dx^2} = \frac{1}{\epsilon_o}\left(\frac{J_p}{v_p} - \frac{J_e}{v_e}\right) \tag{9}$$

$$\frac{d^2V}{dx^2} = \frac{1}{\epsilon_o}\left[J_p\sqrt{\frac{m_p}{2e}}\ \frac{1}{\sqrt{V}} - J_e\sqrt{\frac{m_e}{2e}}\ \frac{1}{\sqrt{v_{eo}^2\frac{m_e}{2e} - V}}\right] \tag{10}$$

defining: $$U^* = v_{eo}^2\ \frac{m_e}{2e} \tag{11}$$

$$a = \frac{J_p}{J_e}\sqrt{\frac{m_p}{m_e}} \tag{12}$$

substituting into equation (10):

$$y = \frac{V}{V_A}\ ;\ y^* = \frac{U^*}{V_A}$$

$$s = \frac{x}{d}\ ;\ s^* = \frac{d^*}{d} \tag{13}$$

and using equation (1), we find:

$$\frac{d^2y}{ds^2} = \frac{4}{9} \frac{J_p}{J_{po}} \left[\frac{1}{\sqrt{y}} - \frac{1}{a} \frac{1}{\sqrt{y^* - y}} \right] \tag{14}$$

For the space between $x = 0$ and $x = d^*$, integrating according to:

$$\frac{1}{2} \frac{d}{ds} \left[\left(\frac{dy}{ds} \right)^2 \right] = \frac{dy}{ds} \frac{d^2y}{ds^2} \tag{15}$$

we integrate twice as follows:

$$\left(\frac{dy}{ds} \right)^2 = \frac{8}{9} \frac{J_p}{J_{po}} \int_0^y \left(\frac{1}{\sqrt{y}} - \frac{\frac{1}{a}}{\sqrt{y^* - y}} \right) dy \tag{16}$$

to integrate with limits between 0 and 1 we change the variable

$$\mu = \frac{y}{y^*} \; ; \tag{17}$$

and thus:

$$\frac{d\mu}{ds} = \frac{4}{3} y^{*-3/4} \sqrt{\frac{J_p}{J_{po}}} \left[\sqrt{\mu} + \frac{1}{a} \left(\sqrt{1 - \mu} - 1 \right) \right]^{1/2} \tag{18}$$

Integrating again:

$$\int_0^{s^*} ds = \frac{3}{4} y^{*3/4} \sqrt{\frac{J_{po}}{J_p}} \int_0^1 \frac{d\mu}{\left[\sqrt{\mu} + \frac{1}{a} \left(\sqrt{1 - \mu} - 1 \right) \right]^{1/2}} \tag{19}$$

$$s^* = y^{*3/4} \sqrt{\frac{J_{po}}{J_p}} \; h\left(\mu, \frac{1}{a} \right) \tag{20}$$

where $h(\mu, \frac{1}{a})$ is $\frac{3}{4}$ of the right side integral. This integral was solved for a similar case in [3].

Solving now for the space between d^* and d, $(a = \infty)$, equation (14) becomes:

$$\frac{d^2y}{ds^2} = \frac{4}{9} \frac{J_p}{J_{po}} \frac{1}{\sqrt{y}} \tag{21}$$

The first integration gives

$$\left(\frac{dy}{ds}\right)^2 = \frac{8}{9} \frac{J_p}{J_{po}} 2y^{1/2} + C \tag{22}$$

The evaluation of C can be obtained from equation (16) after integrating for $s = s^*$, that is:

$$\left(\frac{dy}{ds}\right)^2 \Bigg|_{s = s^*} = \frac{16}{9} \frac{J_p}{J_{po}} y^{*1/2} \left(1 - \frac{1}{a}\right) \tag{23}$$

$$C = -2y^{*1/2} \frac{1}{a} \frac{8}{9} \frac{J_p}{J_{po}} \tag{24}$$

Substituting in equation (22) and integrating again:

$$\int_{s^*}^{1} ds = \frac{3}{4} \left(\frac{J_{po}}{J_p}\right)^{1/2} \int_{y^*}^{1} \frac{dy}{\left[y^{1/2} - \frac{1}{a} y^{*1/2}\right]^{1/2}} \tag{25}$$

$$1 - s^* = \left(\frac{J_{po}}{J_p}\right)^{1/2} R\left(y^*, \frac{1}{a}\right) \tag{26}$$

where $R\left(y^*, \frac{1}{a}\right)$ can be solved substituting: $y = t^2$.

$$R\left(y^*, \frac{1}{a}\right) = \frac{3}{4} \, 2 \int_{\sqrt{y^*}}^{1} \frac{t \, dt}{\sqrt{t - \frac{1}{a}\sqrt{y^*}}} \tag{27}$$

$$R\left(y^*, \frac{1}{a}\right) = \left(\frac{2}{a}\sqrt{y^*} + 1\right)\sqrt{1 - \frac{1}{a}\sqrt{y^*}} - y^{*\frac{3}{4}} \left(1 + \frac{2}{a}\right)\sqrt{1 - \frac{1}{a}} \tag{28}$$

Solving for the case $a = 1$, the expression for $R(y^*, 1)$ becomes

$$R(y^*, 1) = (2\sqrt{y^*} + 1)\sqrt{1 - \sqrt{y^*}} \tag{29}$$

$a = 1$, stands for equal amount of space charges in the space between $x = o$ and $x = d^*$. For the case of cesium atoms the value of $\sqrt{\frac{mp}{me}}$ is about 500 (see footnote 2).

Therefore, an electron current density 500 times the ion current density, is necessary to approach the value $a = 1$. Thus, we have two equations, (20) and (26) with the unknown s^*. Substituting equation (20) in (26) we obtain:

$$\frac{J_p}{J_{po}} = \left(y^{*\frac{3}{4}} h\left(\mu; \frac{1}{a}\right) + R\left(y^*, \frac{1}{a}\right) \right)^2 \qquad (30)$$

The value of $h(1,1)$ was evaluated in [2] and [3] and is 1.36134. Equation (30) becomes:

$$\frac{J_p}{J_{po}} = \left[1.36134\, y^{*\frac{3}{4}} + R(y^*, 1) \right]^2 \qquad (31)$$

---

[2] Electron mass: $m_e = 9.11 \times 10^{-28} g$

Cs - ion mass: $m_p = (Z + N)1837\, m_e$

$$\sqrt{\frac{m_p}{m_e}} = \sqrt{244,321}$$

$$a = 494.28 \frac{J_p}{J_e}$$

EVALUATION OF J_p/J_{po}

The function $(J_p/J_{po}) = f(y^*)$ was evaluated for the case of $a = 1$. This case represents a very large electron space-charge.

Table I shows the program and the results obtained.

Figure 3 shows that the current density increase as a function of the dimensionless kinetic energy of the secondary electrons, $y^* = U^*/V_A$. A maximal current increase of 4.5725 is obtained when the secondary electrons have a kinetic energy of 0.60 with respect to the applied acceleration potential.

TABLE I

SOURCE PROGRAM

```
C  CURRENT INCREASE IN AMBIPOLAR SPACE CHARGE
       Y = 0.0
       X = Y-1.0
   11  IF (X)  1, 1, 2
    1  D = (1.36134*SQRTF(SQRTF(Y**3)) + (2.*SQRTF(Y) + 1.)*SQRTF(1.-SQRTF(Y)))**2
   10  FORMAT (2F10.6)
       PRINT 10,  Y,  D
       PUNCH 10,  Y,  D
       Y = Y + 0.05
       GO TO 11
    2  END
```

TABLE I (cont'd)

RESULT

y^*	J_p/J_{po}
0.000000	1.000000
.050000	2.013929
.100000	2.534369
.150000	2.948747
.200000	3.296529
.250000	3.592995
.300000	3.845727
.350000	4.058865
.400000	4.234664
.450000	4.374175
.500000	4.477542
.550000	4.544128
.600000	4.572500
.650000	4.560294
.700000	4.503924
.750000	4.398000
.800000	4.234159
.850000	3.998455
.900000	3.664365
.950000	3.165833
1.000000	1.853246

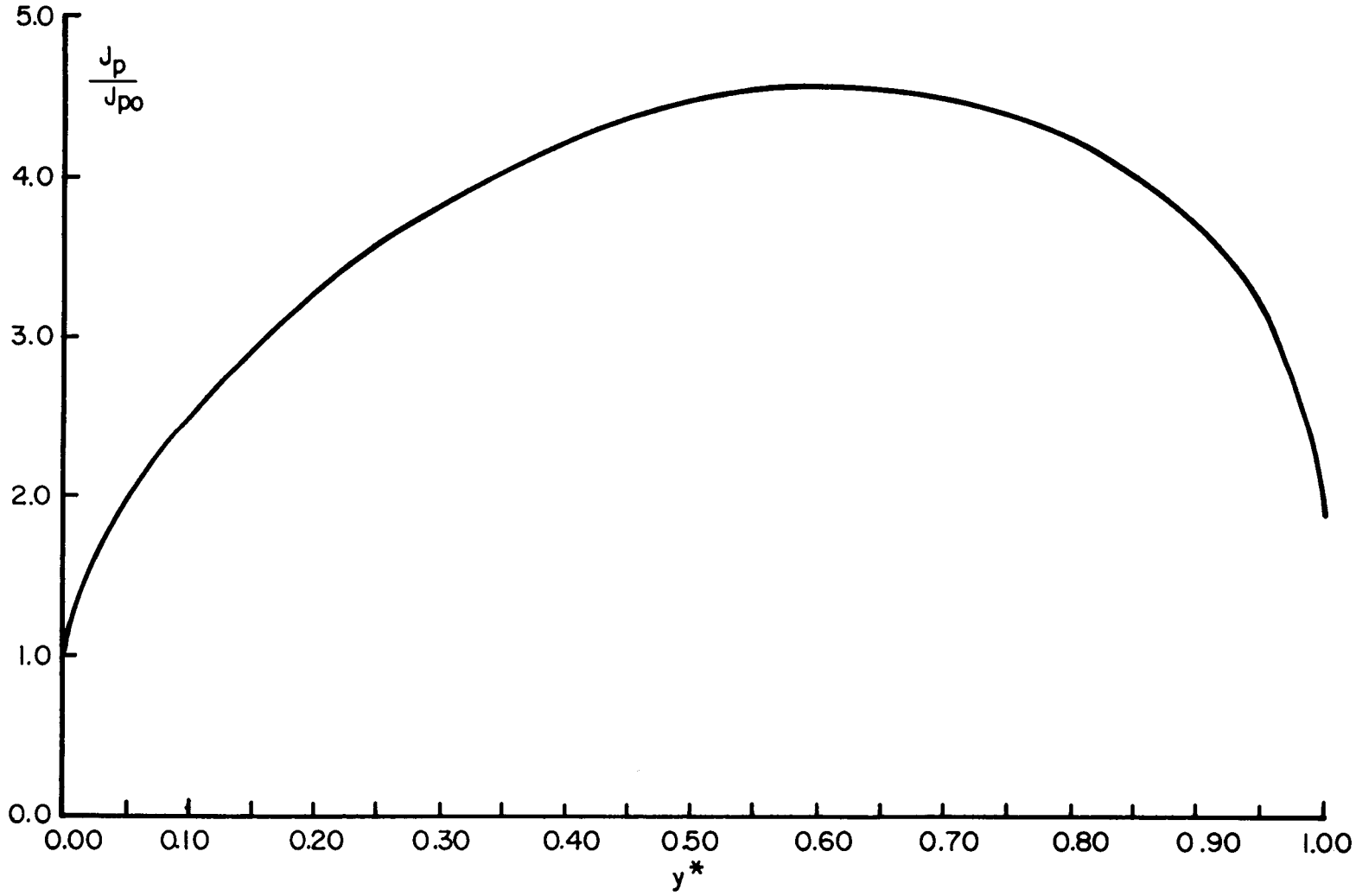

FIG. 3 CURRENT DENSITY INCREASE IN FUNCTION OF THE DIMENSIONLESS KINETIC ENERGY OF THE SECONDARY ELECTRONS

CONCLUSION

The problem considered herein differs from that considered by Langmuir [2] in two respects: first, there is as many electrons as ions present, while Langmuir is considering an electron rich system only; second, the present analysis is concerned with the acceleration of ions rather than electrons.

From the model adopted for this analysis, and its evaluation, it seems improbable that the large amount of power observed at the output of the ion beam-thrustor [1] is due only to the effect of space charge compensation by the secondary emission.

It is possible that the observed phenomena could have been helped by a second production of ions in the space between the ion-emitter and the accelerator system. This, of course, could only happen if enough molecular cesium flows out of the cesium boiler without being ionized while crossing the porous tungsten. If this was the case, the large current increase might have been due to collision ionization of the free cesium molecules by the primary electrons. The electrons were emitted in a high accelerating potential field, sufficient to ionize the neutral cesium.

Another supporting argument for this assumption is the impingement effect observed (see Fig. 13 in [1]). The impingement of the outside ions of the beam with the accelerator's edge could cause secondary emission. These secondary electrons find a high

potential accelerating field toward the ion-emitter and thus possibly collide with neutral cesium atoms in their trajectory to the ion-emitter. Because that can occur in any place inside of the accelerator system, the ionized atoms are not forced to cross the space charge limitation zone resulting in a further increase of ions current.

Recently, a paper by Walton L. Howes (Lewis Research Center, Cleveland, Ohio, NASA Technical Note, NASA TN D-2425, of August, 1964, was published showing that the current increase in a space with ambipolar charges can be 25 times greater, if the initial kinetic energy of the charges is about 5 times its potential energy. Since these initial conditions appear inconsistent with the observed phenomenon no consideration was given to it.

ANNOTATED BIBLIOGRAPHY

[1] Baldwin, L. V. and V. A. Sandborn, Hot-Wire Calorimeter Study of Ion Production and Acceleration. AIAA Journal, Volume 2, Number 4. April, 1964. pp. 660-666.

[2] Langmuir, Irving. The Interaction of Electron and Positive Ion Space Charges in Cathode Sheets. Physical Review 33, Number 6, June, 1929. pp. 954-989.

[3] Müller-Lübeck, K., Über die ambipolare Raumladungsströmung bei ebenen Elektroden. Zeitschrift für Angewandte Physik, Volume 3, Number 11, 1951. pp. 409-415.

[4] Rothe, H. and Werner Klenn, Grundlagen und Kennlinien der Elektronenröhren. Leipzig. Akademische Verlagsgesellschaft, 1948.

[5] Spanenberg, K. R., Vacuum Tubes. New York: McGraw-Hill, 1948.

[6] Kunz, Kaiser S., Numerical Analysis. New York: McGraw-Hill, 1957.

[7] Grabbe, E. M., S. Ramo and D. E. Worldridge, Handbook of Automation, Computation and Control. Volume 1; New York: J. Wiley and Sons, 1958.

SOURCES CONSULTED:

1. Azaroff, L. V. and J. J. Brophy, Electronic Processes in Materials. New York: McGraw-Hill, 1963.

2. Baldwin, L. V. and V. A. Sandborn, Hot-Wire Calorimeter Study of Ion Production and Acceleration. AIAA Journal, Volume 2, Number 4, April, 1964. pp. 660-666.

3. Bruining, H., Physics and Applications of Secondary Electron Emission. New York: McGraw-Hill, 1954.

4. Campbell, William G., A Form Book for Thesis Writing. New York: Houghton Mifflin Company, 1939.

5. Grabbe, E. M., S. Ramo and D. E. Worldridge, Handbook of Automation, Computation and Control. 3 volumes; New York: J. Wiley and Sons, 1958.

6. Hamza, V. and E. Richley, Numerical Solution of Two-Dimensional Poisson Equation: Theory and Application to Electrostatic Ion-Engine Analysis. NASA Technical Note E-1323, October, 1962.

7. _____, Numerical Evaluation of Ion-Thrustor Optics. NASA Technical Note D-1665, May, 1963.

8. Jahnke, E. and F. Emde, Tables of Functions with Formulae and Curves. Fourth edition; New York: Dover Publications, 1945.

9. Jonker, J. L. H., On the Theory of Secondary Electron Emission. Philips Research Reports 7, 1-20, February, 1952.

10. Kunz, Kaiser S., Numerical Analysis. New York: McGraw-Hill, 1957.

11. Kuskevics, G., Criteria and a Graphical Method for Optimization of Cesium Surface Ionizer Materials. Electro-Optical-System, Inc., Pasadena, California: Research Report No.3, January, 1962.

12. Langmuir, Irving. The Interaction of Electron and Positive Ion Space Charges in Cathode Sheets. Physical Review 33, No.6, June, 1929, pp. 954-989.

SOURCES CONSULTED cont'd:

13. Langmuir, D. B., E. Stuhlinger and J. M. Sellen, Jr., Electrostatic Propulsion. 5 volumes; New York: Academic Press, 1961.

14. Lockwood, D. L., and V. Hamza, Space-charge-flow Theory and Electrode Design for Electrostatic Rocket Engines. NASA Technical Note D-1461, December, 1962.

15. Müller-Lübeck, K., Über die ambipolare Raumladungsströmung bei ebenen Elektroden. Zeitschrift für Angewandte Physik, volume 3, number 11, 1951, pp. 409-415.

16. Richley, E. and W. R. Mickelsen, Effects of Molecular Flow in Plasma Generation and some Analyses of Space Charge Flow in Ion Acceleration. NASA Technical Preprint 21-63, January 1964.

17. Rint, C., Handbuch für Hochfrequenz und Elektrotechnik. 6 Bände; Berlin. Verlag für Radio-Foto Kinotechnik GmbH. 1952.

18. Rothe, H. and Werner Klenn, Grundlagen und Kennlinien der Elektronenröhren. Leipzig. Akademische Verlagsgesellschaft, 1948.

19. Spanenberg, K. R., Vacuum Tubes. New York: McGraw-Hill, 1948.

20. _____, Fundamentals of Electron Devices. New York: McGraw-Hill, 1957.

21. Taylor, J. B. and I. Langmuir, The Evaporation of Atoms, Ions, and Electrons from Caesium Films on Tungsten. Physical Review 44, 1933, pp. 423.

22. Zworykin, V. K. and G. A. Morton, Television. Second edition; New York: J. Wiley and Sons, 1954.

APPENDIX

METHODS FOR CALCULATING ELECTRIC FIELDS CONTAINING SPACE-CHARGE AND SPACE-CHARGE-FREE ZONES

To obtain the potential distribution in a space-charge field between two infinite parallel plates it is necessary to solve Poisson's equation in only one dimension [4]:

$$\frac{d^2U}{dx^2} = - \frac{\rho_i}{\epsilon_o} \tag{1}$$

ρ_i is a function of U, such that

$$\frac{d^2U}{dx^2} = - C_1 \frac{1}{\sqrt{U}} \tag{2}$$

where C_1 is a constant for a given case.

The use of a digital computer simplifies considerably the work necessary to find the potential distribution, and increases the accuracy. This problem was solved with a digital computer, IBM 1620, using the language Fortran II. Figure 4 shows two parallel plates containing space-charge and space-charge-free zones. The two horizontal lines represent the parallel plates. It is assumed that they are infinite to the left and to the right. An ion beam goes from the zero potential plate to the -100 volt plate, only at the center of the system. Thus, in this area ρ_i will be different from zero [4]. Equation (3) gives the function of ρ_i

$$\rho_i = J \sqrt{\frac{m}{2e}} \cdot \sqrt{\frac{1}{U}} \tag{3}$$

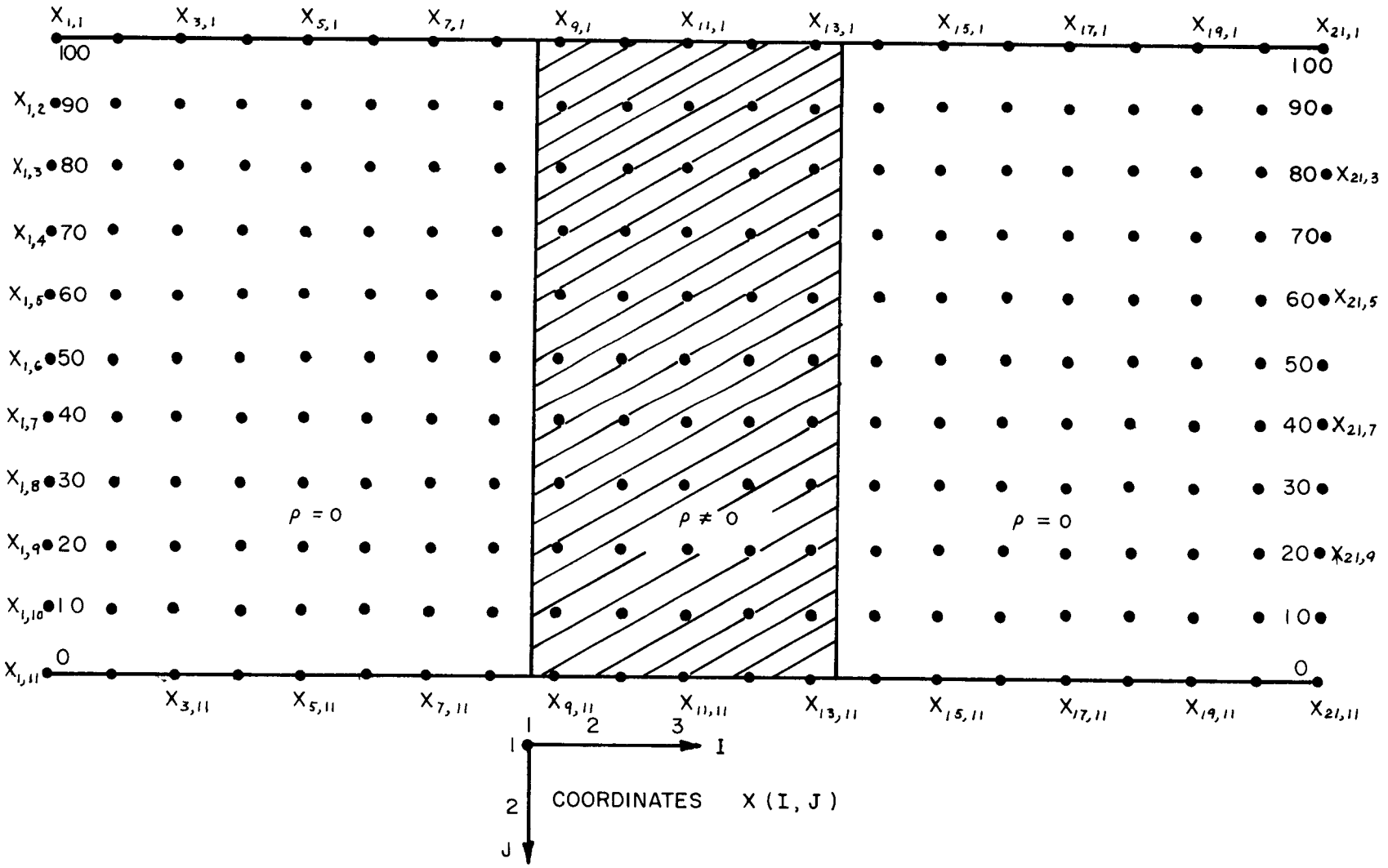

FIG. 4 NET OF POINTS FOR TWO INFINE PARALLEL

where: J is the current density, m is the ion mass, and e is the ions charge. On the left and right side of the beam, ρ_i is equal to zero.

An iterative method was used to calculate the potential lines. The function to be computed is equation (4). It is termed the Liebmann improvement formula of Poisson's equation ([6] page 317 and 318).

The field is defined by a net of points as shown in Figure 4. Each of the points is a location in the program, and the values of the points are their corresponding potentials. By averaging the four adjacent potentials as shown in equation (4):

$$U_{i,j} = \frac{U_{(i-1,\,j)} + U_{(i+1,\,j)} + U_{(i,\,j-1)} + U_{(i,\,j+1)} - \rho_i \epsilon_o}{4} \quad (4)$$

the new value will be obtained for the point under consideration. The subindices i in equation (4) refer to the columns of points in the net of Figure 4. The subindices j refer to the rows.

At infinity in both directions, left and right, the potential gradient is constant. To simulate this situation, fixed potentials will be assigned with a constant gradient to the left-most and right-most column of the net. This is only an approximation, because the constant gradient is very far from the space-charge zone. The error of this approximation can be reduced by setting the constant gradient farther from the space-charge zone as in the case of Figure 4. The iterative method used here is fully justified as follows:

Poisson's equation for a two dimensional field is

$$\frac{\partial^2 U}{\partial z^2} + \frac{\partial^2 U}{\partial y^2} = \frac{-\rho}{\epsilon_o} \tag{15}$$

Using increments for the first derivative, it will be obtained ([6], [7]):

$$\frac{\partial U}{\partial z} = \frac{U_{(z + \Delta z,\, y)} - U_{(z,\, y)}}{\Delta z}$$

for the second derivative:

$$\frac{\partial^2 U}{\partial z^2} = \frac{U_{(z + 2\Delta z,\, y)} - U_{(z + \Delta z,\, y)} - U_{(z + \Delta z,\, y)} + U_{(z,y)}}{(\Delta z)^2}$$

or:

$$\frac{\partial^2 U}{\partial z^2} = \frac{U_{(z + \Delta z,\, y)} - 2U_{(z,\, y)} + U_{(z - \Delta z,\, y)}}{(\Delta z)^2}$$

and hence:

$$\frac{\partial^2 U}{\partial y^2} = \frac{U_{(z,\, y + \Delta y)} - 2U_{(z,\, y)} + U_{(z,\, y - \Delta y)}}{(\Delta y)^2}$$

By taking the increments $|\Delta z| = |\Delta y| = \frac{1}{p}$, substituting in equation (15) and calling $z = i$, and $y = j$, the following is obtained:

$$U_{(i + 1,\, j)} + U_{(i - 1,\, j)} + U_{(i,\, j - 1)} + U_{(i,\, j + 1)} - 4U_{(i,\, j)} = -\frac{\rho}{\epsilon_o} \frac{1}{p^2}$$

This equation can be written in the form of equation (4) with only the difference of $1/p^2$. This factor affects the accuracy of the method. In the case of a net formed by 10 x 10 points:

$$\frac{1}{p^2} = \frac{1}{100} \quad .$$

Equation (4) is used here to obtain a field described by equation (1). This is the case where a space charge is created by an emission, and the potential function follows a "4/3 power law" given by

equation (5).

$$U_x = U_0 \left(\frac{x}{d}\right)^{4/3} \qquad (5)$$

It is assumed in equations (1) and (5) that the initial velocity of the ions is zero, however this is not the real case.

(I) THE PROGRAM

Table II shows the source program, the data, and the results of the processing of the condensed program.

Figure 5 shows the flow chart used for this program. The program starts by setting the boundary values of 100 for the upper plate, zero for the lower, and the constant gradient values at all places. This is the case of Laplace's equation. The accelerating potential for ions is negative and the upper plate should be -100, but this change of sign can be made in the results. The arithmetic operation to be evaluated is given by equation (4). Prior to calculating any potential $U_{i,j}$ (in the program called X(I,J)), the program has two decision-statements in order to set ρ_i equal to, or different from, zero. For the central columns, between column 9 and 13, ρ_i is made different from zero. The iterative approximations are made 20 times, and the results are punched in cards. Each card will contain half a row. The complete row will not be punched because the expected field lines are completely symmetrical with respect to the central line. A typing statement for X(11, 6) equivalent to the center

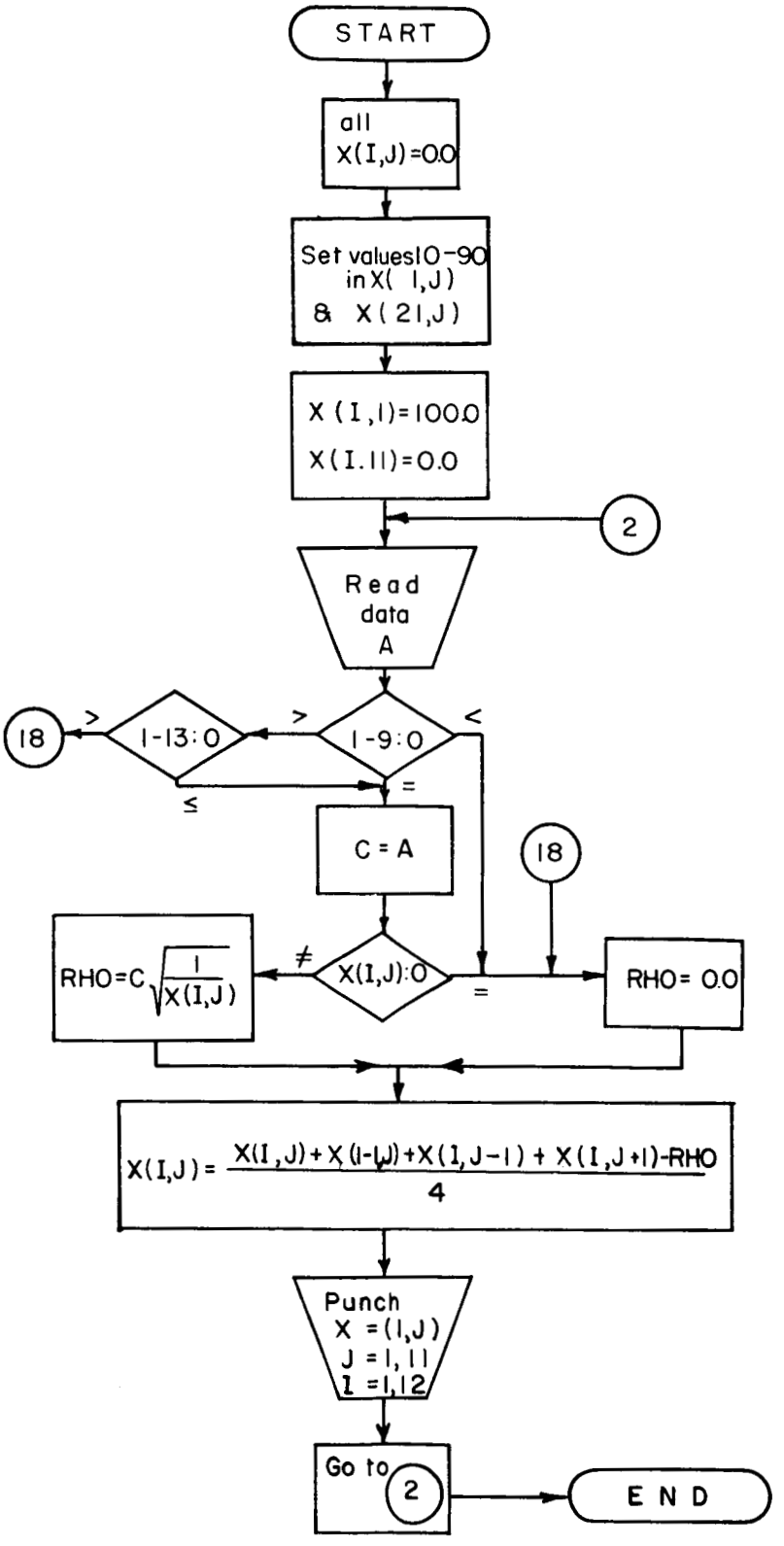

FIG. 5 FLOW-CHART FOR PROGRAM (I)

of the system, makes visible, after each iteration, the change from the previously calculated value, and therefore, the reduction of error. The same program and configuration can be used for an ion beam or an electron beam. The distinction can be made in the evaluation of the data obtained from the computer.

The processed equation is:

$$X_{(I,J)} = \frac{X_{(I-1,J)} + X_{(I+1,J)} + X_{(I,J-1)} + X_{(I,J+1)} - RHO}{4} \quad (5)$$

and

$$RHO = C\sqrt{\frac{1}{X_{(I,J)}}} \quad (6)$$

but to satisfy Poisson's equation, it must be:

$$RHO = \frac{\rho}{\epsilon_o}\ \frac{1}{p_1 p_2} \quad (7)$$

where p_1 and p_2 are the dimensions of the net. In this case $\frac{1}{p_1 p_2} = \frac{1}{200}$. Considering equations (3), (6) and (7),

$$C = \frac{1}{200}\ \frac{J}{\epsilon_o}\sqrt{\frac{m_e}{2e}} \quad \text{, where} \quad (8)$$

$\epsilon_o = 8.86 \times 10^{-14}\ \left[V^{-1}\ A\ sec\ cm^{-1}\right]$. For the case of an electron beam

$$\sqrt{\frac{m_e}{2e}} \approx 1.683 \times 10^{-8}\ \left[V^{1/2}\ sec\ cm^{-1}\right] \quad (9)$$

Hence,

$$\frac{1}{\epsilon_o}\sqrt{\frac{m_e}{2e}} = 1.9 \times 10^5 \left[V^{3/2} A^{-1} \right]$$

and so:

$$C \approx J \times 10^3 .$$

Thus, if we enter with the data card the value of 10^{-3}, it will be read and located in A. When $\rho \neq 0$, C will be 10^{-3} and that corresponds to a current density of $J = 1$ A/cm^2. Correspondingly, a current density of $J = 10$ mA/cm^2, will be represented by a data card with the value of 10.

In the case of an ion-beam these numbers are different. Equation (9) for cesium atoms will have the value of:

$$\frac{1}{\epsilon_o}\sqrt{\frac{m_i}{2e}} = 0.806 \times 10^8 \left[\frac{V^{3/2}}{A} \right]$$

Thus,

$$C = \frac{10^8}{200} \times J_i = 5 \times 10^5 \times J_i$$

This result shows that the ion current is 500 times less than an electron current for the same potential distribution. Figure 6 shows the obtained field lines, and Figure 7 shows the potential distribution of the center of the system.

This case corresponds to an electron current density of: 10mA/cm^2 and an ion current density of: 20μA/cm^2.

This is the case of a space-charge between electrodes with zero electric field close to the emission surface. That means, that

(cont'd page 35)

TABLE II

```
C  POISSON AND LAPLACE EQUATION IN SAME SPACE, PARALLEL PLATES,
      DIMENSION X(21,11)
      DO  1  I = 1,21
      X(I,1) = 100.0
      X(I,2) = 90.0
      X(I,3) = 80.0
      X(I,4) = 70.0
      X(I,5) = 60.0
      X(I,6) = 50.0
      X(I,7) = 40.0
      X(I,8) = 30.0
      X(I,9) = 20.0
      X(I,10) = 10.0
    1 X(I,11) = 0.0
   10 FORMAT (F6.3)
    2 READ  10,A
      DO  11  L = 1,20
    3 FORMAT (F8.1)
      PRINT  3, X(11,6)
      DO  11  J = 2,10
      DO  11  I = 2,20
     IF (I-9)  18,5,6
    5   C = A
     GO  TO  9
    6 IF  (I-13)  5,5,18
   18 RHO = 0.0
```

continued next page

TABLE II (cont'd)

```
      GO TO 11
 9    RHO = C*SQRTF  (1.00/x(I,J))
11    X(I,J) = (X(I-1,J) + X(I+1,J) + X(I,J - 1)+ X(I,J+1) - RHO) /4.0
      DO  13  J = 1,11
12    FORMAT (12F6.1)
13    PUNCH  12,X(1,J),X(2,J),X(3,J),X(4,J),X(5,J),X(6,J),X(7,J(,X(8,J)
    1  X(9,J),X(10,J),X(11,J),X(12,J)
14    GO TO 2
      END
```

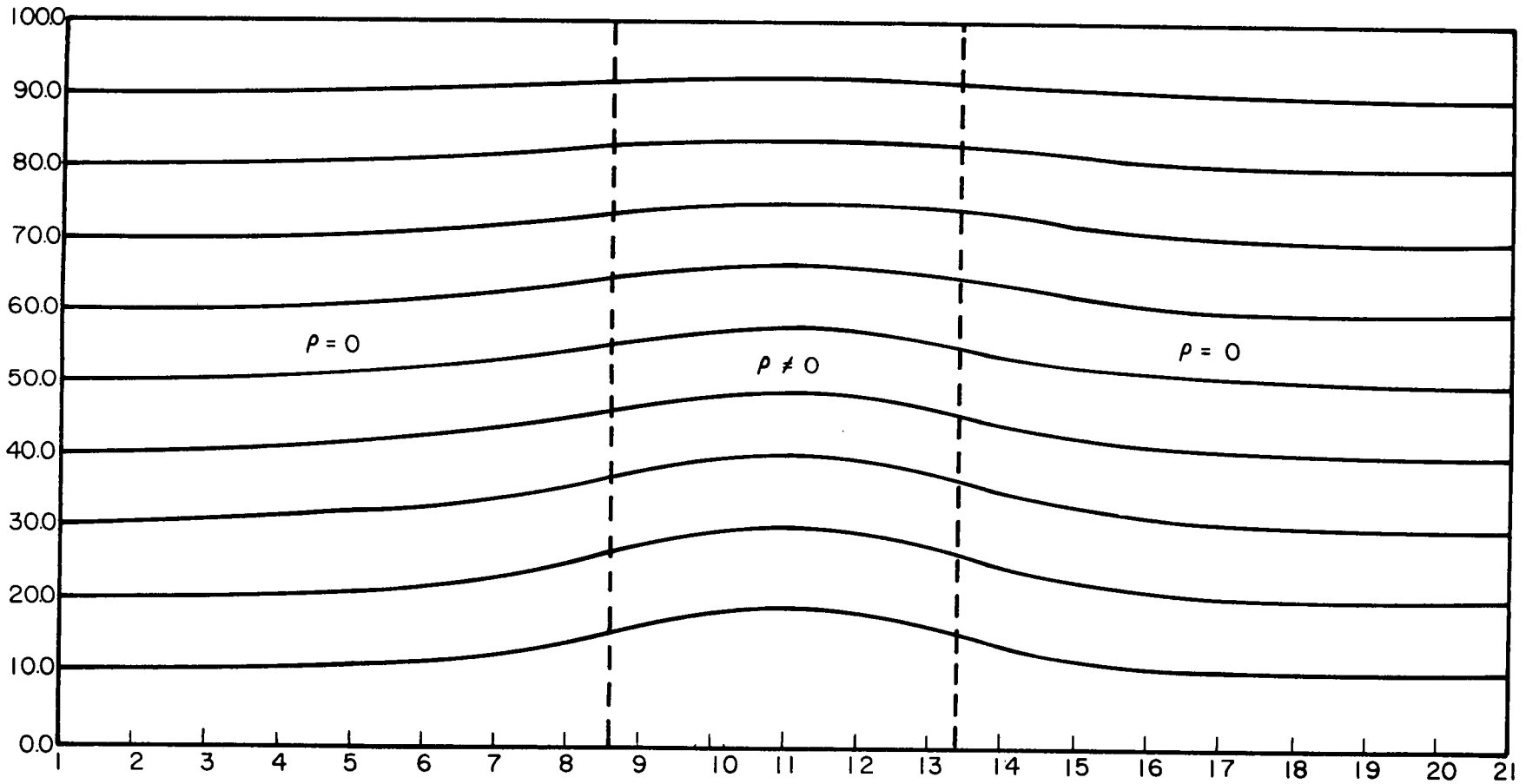

FIG. 6 POTENTIAL FIELD FOR C=10

TABLE II (cont'd)

POISSON EQUATION FOR C = 10

I: 1	2	3	4	5	6	7	8	9	10	11	12
100.0	100.0	100.0	100.0	100.0	100.0	100.0	100.0	100.0	100.0	100.0	100.0
90.0	89.9	89.9	89.9	89.7	89.5	89.2	88.7	87.9	87.5	87.3	87.4
80.0	79.9	79.8	79.7	79.5	79.1	78.6	77.7	76.4	75.6	75.4	75.5
70.0	69.9	69.8	69.6	69.3	68.8	68.0	66.8	65.2	64.2	63.8	64.1
60.0	59.9	59.7	59.5	59.1	58.5	57.5	56.1	54.2	53.0	52.6	52.8
50.0	49.9	49.7	49.4	49.0	48.3	47.2	45.6	43.4	42.1	41.5	41.9
40.0	39.8	39.7	39.4	38.9	38.2	37.0	35.3	32.8	31.4	30.8	31.2
30.0	29.9	29.7	29.4	29.0	28.3	27.1	25.3	22.7	21.1	20.5	20.9
20.0	19.9	19.7	19.5	19.2	18.6	17.6	15.9	13.2	11.6	11.0	11.4
10.0	9.9	9.8	9.7	9.5	9.2	8.5	7.4	5.0	3.7	3.2	3.6
0.0	0.0	0.0	0.0	0.0	0.0	0.0	0.0	0.0	0.0	0.0	0.0

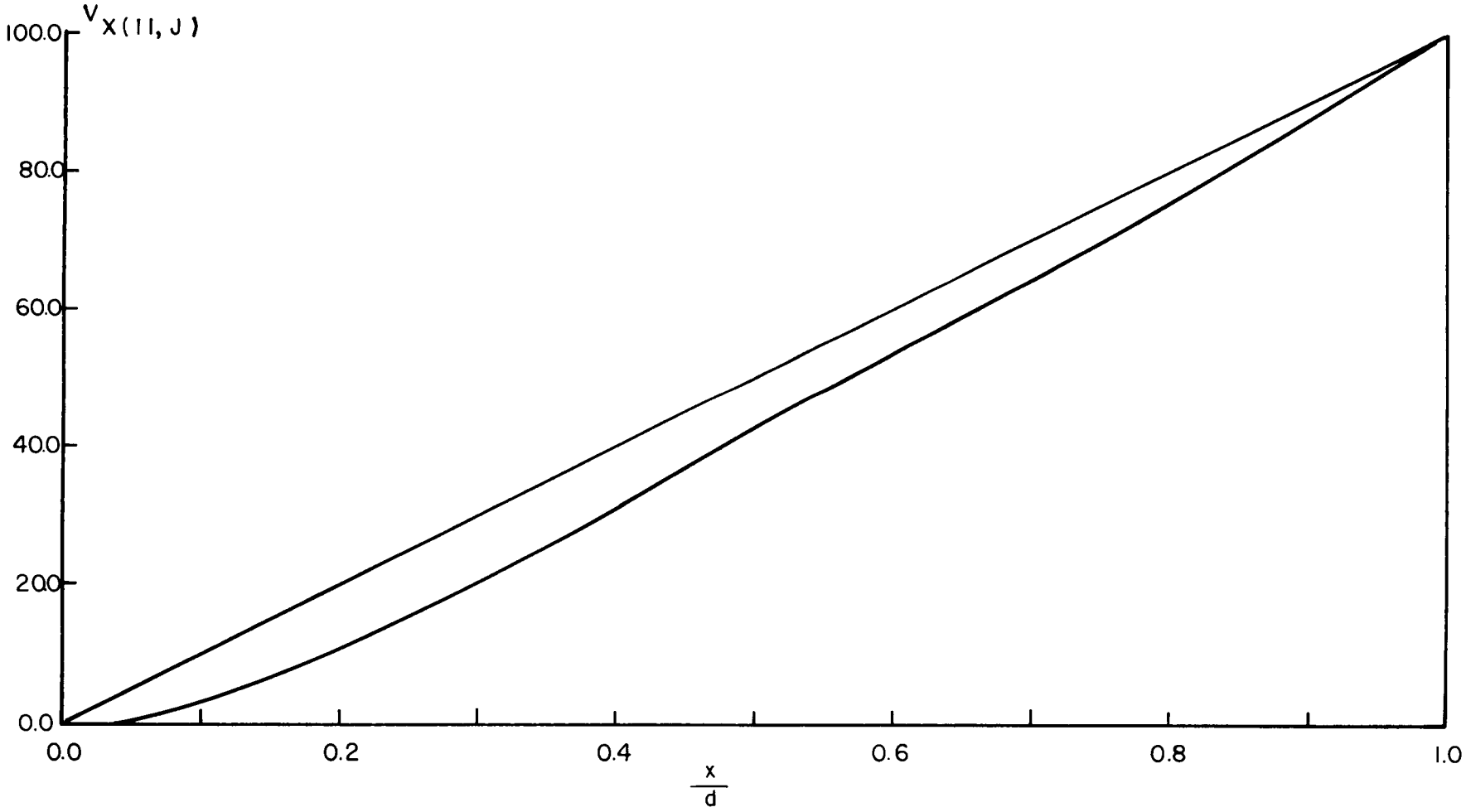

FIG. 7 POTENTIAL DISTRIBUTION AT THE CENTER OF THE SYSTEM

the space charges have zero initial velocity in the emitter. Thus, no potential-minimum exists between the electrodes. An increase of the emitter temperature would cause an increase of the emitted current, and therefore, this creates a "virtual cathode" with a minimum potential. The iterative procedure used here with $\rho = \frac{C}{\sqrt{U}}$ corresponds only to the "4/3 law", that is, only to the zone between the "virtual cathode" and the collector.

(II) The program for this case was changed, so that one of the points was held to a constant potential. The point chosen was the X(11, 6) and it was held to 50.0, that is, the value corresponding to the Laplace equation for that point.

For the control of the successive approximations, the point X(11,10) was chosen, that is, the point with the highest rate of change.

To improve the iteration and to estimate the errors, the number of iterations was increased to 50. Table III shows the new source program, the results of the computation and the potential lines. They also show the values of the point X(11,10), and the differences between the values of two consecutive iterations. Figures 10 and 11 show the corresponding graphs in function of the number of iterations. In Figure 10, it is possible to see that X(11,10) approaches the value of 2, and after 50 iterations it is possible to obtain results with less that 10% error, with respect to the end value. Figure 11 shows that the differences between successive iterations are so small

after 50 iterations that a much better result is obtainable only by increasing the number of iterations to 500, 1000 or more.

(III) Given a constant potential between emitter and collector, an increase of the emitter temperature produces a potential minimum close to the emitter. This can only occur when the emitted charges have an initial velocity (thermal velocity) different from zero.

The energy of the emitted charges may have a Maxwellian-distribution, and thus the potential function between emitter and potential minimum does not follow the "4/3 law", ("Childs-Langmuir-space-charge law" solved for the potential), considered above.

Only under the assumption of a uniform initial velocity, is it possible to make an approximation to the "4/3 law" in this zone.

The program shown in Table IV is similar to the one shown in Part (II). Here the evaluation of RHO, if X(I,J) is negative, is modified. Figure 12 shows the potential lines for this case and Figure 13 the potential distribution in the center of the system.

TABLE III

```
C  POISSON AND LAPLACE EQUATION IN SAME SPACE, DISTURBANCE,
      DIMENSION X(21,11)
      DO 1 I = 1,21
      X(I,1) = 100.0
      X(I,2) = 90.0
      X(I,3) = 80.0
      X(I,4) = 70.0
      X(I,5) = 60.0
      X(I,6) = 50.0
      X(I,7) = 40.0
      X(I,8) = 30.0
      X(I,9) = 20.0
      X(I,10) = 10.0
    1 X(I,11) = 0.0
   10 FORMAT (F6.3)
    2 READ 10,A
      DO 11 L = 1,50
    3 FORMAT (F7.3)
      PRINT 3, X(11,10)
      DO 11 J = 2,10
      DO 11 I = 2,20
      X(11,6) = 50.0
      IF (I-9) 18,5,6
    5 C = A
      GO TO 9
```

continued next page

TABLE III (cont'd)

```
 6  IF (I-13) 5,5,18
18  RHO = 0.0
    GO TO 11
 9  RHO = C*SQRTF (1.00/X(I,J))
11  X(I,J) = (X(I - 1,J) + X(I+1,J) + X(I,J - 1) + X(I,J+1) - RHO)/4.0
    DO 13 J = 1,11
12  FORMAT (12F6.1)
13  PUNCH 12,X(1,J),X(2,J),X(3,J),X(4,J),X(5,J),X(6,J),X(7,J),X(8,J),
   1 X(9,J),X(10,J),X(11,J),X(12,J)
14  GO TO 2
    END
```

TABLE III (cont'd)

POISSON EQUATION, DISTURBANCE C = 10

100.0	100.0	100.0	100.0	100.0	100.0	100.0	100.0	100.0	100.0	100.0	100.0
90.0	89.9	89.8	89.6	89.5	89.3	89.0	88.5	87.8	87.5	87.4	87.5
80.0	79.8	79.6	79.3	79.0	78.6	78.1	77.4	76.3	75.9	75.8	75.9
70.0	69.7	69.4	69.1	68.7	68.1	67.5	66.6	65.4	65.0	65.1	65.0
60.0	59.6	59.3	58.9	58.4	57.8	57.0	56.0	54.9	54.9	55.9	54.9
50.0	49.6	49.3	48.8	48.3	47.6	46.7	45.6	44.5	45.3	50.0	45.3
40.0	39.6	39.3	38.8	38.3	37.5	36.5	35.2	33.6	33.3	34.2	33.3
30.0	29.7	29.3	28.9	28.4	27.7	26.6	25.1	22.9	22.0	21.9	22.0
20.0	19.7	19.5	19.2	18.8	18.1	17.2	15.7	13.2	11.9	11.6	11.9
10.0	9.8	9.7	9.5	9.3	8.9	8.3	7.2	4.9	3.8	3.4	3.8
0.0	0.0	0.0	0.0	0.0	0.0	0.0	0.0	0.0	0.0	0.0	0.0

TABLE III
(cont'd)

ENTER DATA C = 10

X(11,10)	X(11,10) cont'd
10.000	3.931
8.646	3.893
7.791	3.857
7.161	3.824
6.686	3.794
6.309	3.765
5.999	3.739
5.739	3.714
5.516	3.691
5.323	3.669
5.153	3.649
5.003	3.630
4.870	3.613
4.750	3.597
4.643	3.581
4.545	3.567
4.457	3.554
4.377	3.541
4.303	3.530
4.236	3.519
4.175	3.509
4.118	3.499
4.066	3.491
4.017	3.482
3.973	3.475

TABLE III
(cont'd)
C = 10

X(11,10)	DIFFERENCE	X(11,10)cont'd	DIFFERENCE
8.643			
7.781	1.357	3.259	0.070
7.141	0.862	3.195	0.066
6.651	0.640	3.134	0.064
6.256	0.490	3.076	0.061
5.926	0.395	3.020	0.058
5.643	0.330	2.966	0.056
5.396	0.283	2.914	0.054
5.177	0.247	2.864	0.052
4.980	0.219	2.815	0.050
4.802	0.197	2.768	0.049
4.641	0.178	2.722	0.047
4.492	0.161	2.678	0.046
4.356	0.149	2.635	0.044
4.229	0.136	2.593	0.043
4.111	0.127	2.552	0.042
4.002	0.118	2.512	0.041
3.899	0.109	2.473	0.040
3.803	0.103	2.434	0.039
3.712	0.096	2.397	0.039
3.626	0.091	2.359	0.036
3.545	0.086	2.323	0.038
3.468	0.081	2.286	0.036
3.395	0.077	2.250	0.037
3.325	0.073	2.215	0.035

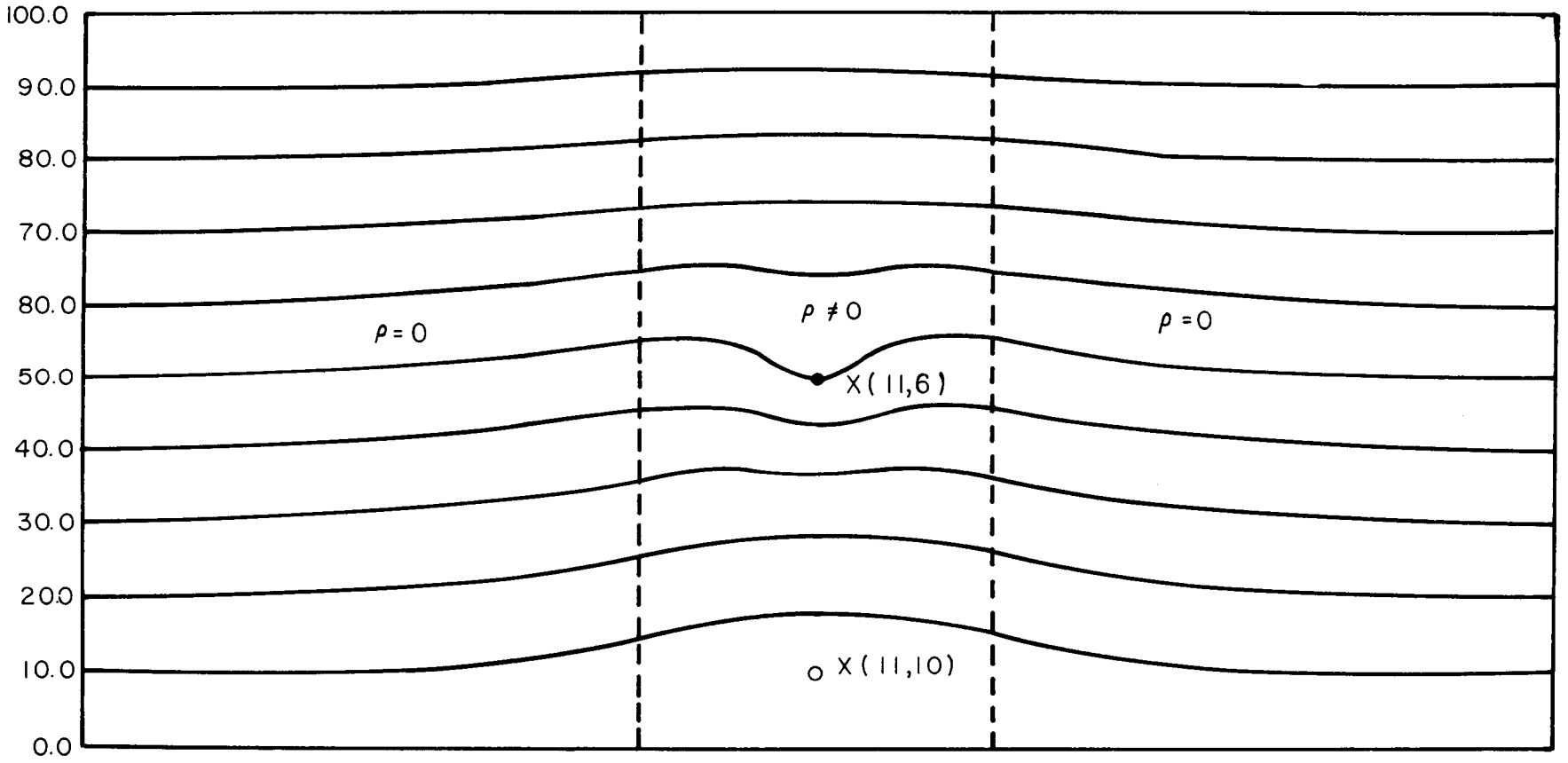

FIG. 8 POTENTIAL FIELD FOR C=10. PROGRAM (II)

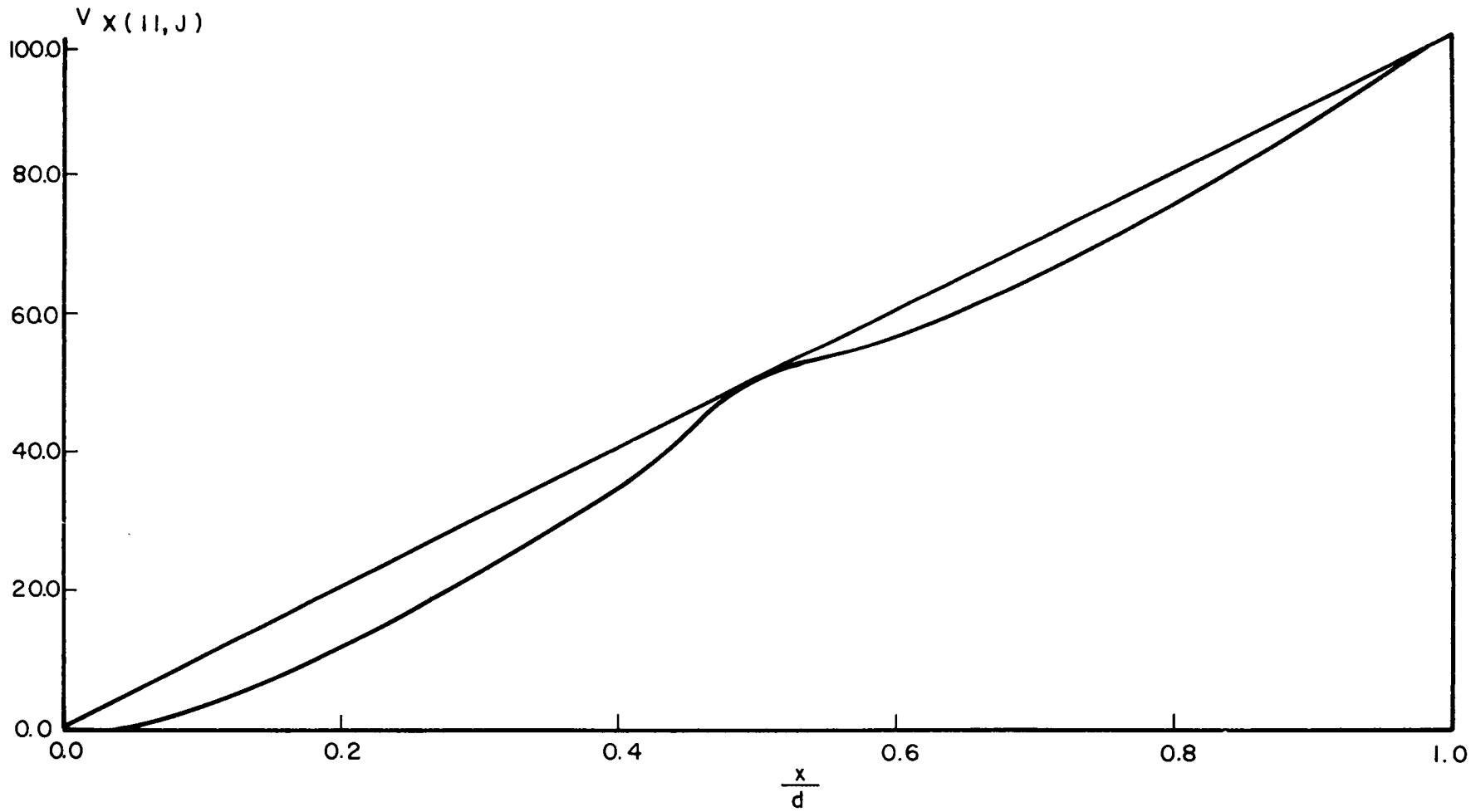

FIG. 9 POTENTIAL DISTRIBUTION. PROGRAM (II)

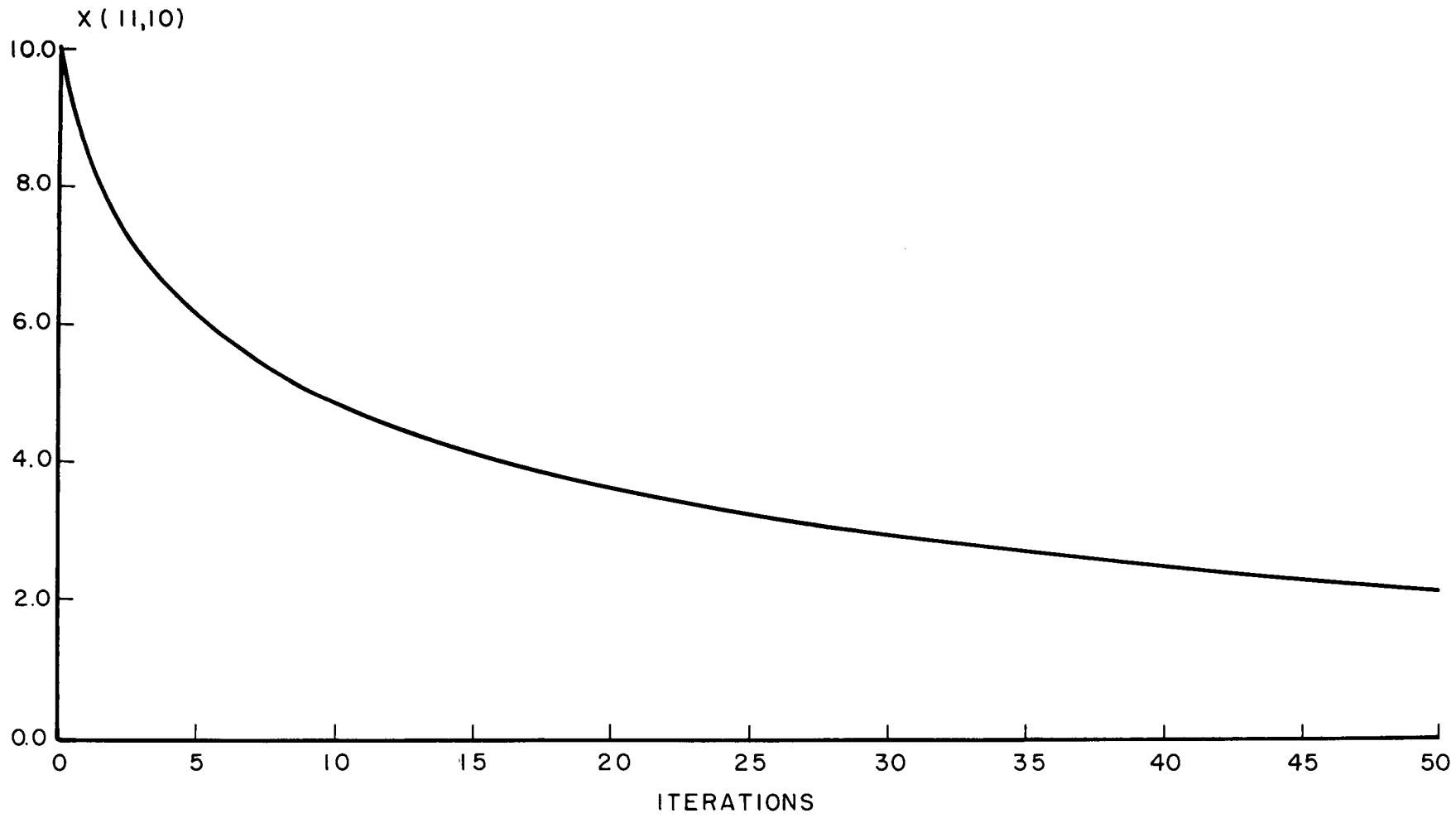

FIG. 10 VALUE OF X (11, 10). PROGRAM (II)

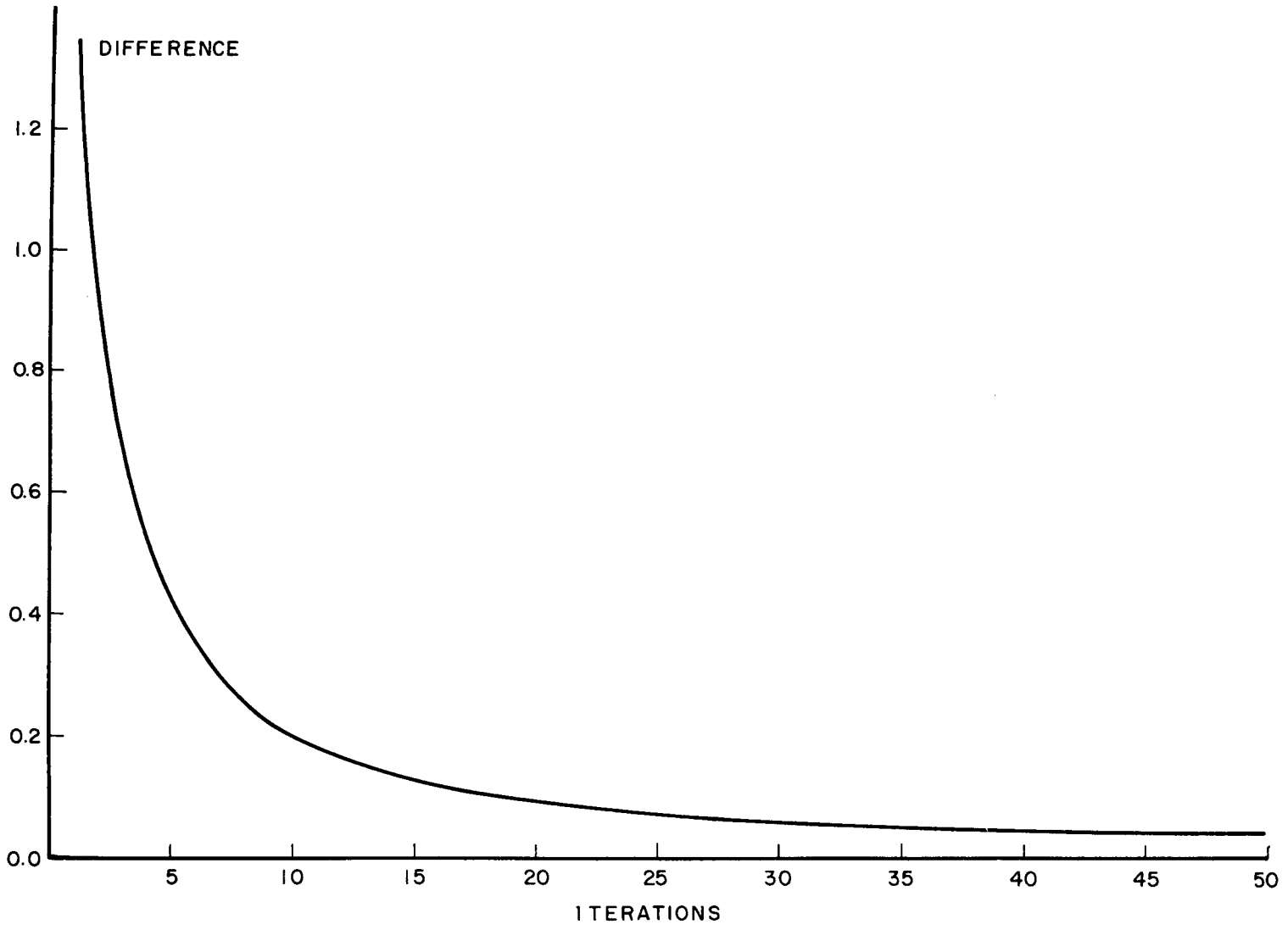

FIG. 11 RATE OF CHANGE OF X (11, 10). PROGRAM (II)

TABLE IV

```
C  POISSON AND LAPLACE EQUATION IN SAME SPACE,
C  DISTURBANCE
       DIMENSION X(21,11)
       DO 1 I = 1,21
       X(I,1) = 100.0
       X(I,2) = 90.0
       X(I,3) = 80.0
       X(I,4) = 70.0
       X(I,5) = 60.0
       X(I,6) = 50.0
       X(I,7) = 40.0
       X(I,8) = 30.0
       X(I,9) = 20.0
       X(I,10) = 10.0
  1    X(I,11) = 0.0
 10    FORMAT (F6.3)
  2    READ 10,A
       DO 11 L = 1,50
  3    FORMAT (F7.3)
       PRINT 3, X(11,10)
       DO 11 J = 2,10
       DO 11 I = 2,20
       X(11,6) = 50.0
       IF (I-9) 18,5,6
  5    C = A
       GO TO 9
```

TABLE IV (cont'd)

```
 6    IF (I-13) 5,5,18
18    RHO = 0.0
      GO TO 11
 9    IF (X(I,J)) 20,19,19
20    RHO = C*SQRTF(1.00/(-X(I,J)))
      GO TO 11
19    RHO = C*SQRTF (1.00/X(I,J))
11    X(I,J) = (X(I-1,J) + X(I+1,J) + X(I,J-1) + X(I,J+1) - RHO) / 4.0
      DO 13 J = 1,11
12    FORMAT (12F6.1)
13    PUNCH 12,X(1,J), X(2,J), X(3,J), X(4,J), X(5,J), X(6,J), X(7,J), X(8,J),
     1 X(9,J), X(10,J), X(11,J), X(12,J)
14    GO TO 2
      END
```

TABLE IV (cont'd)

C = 15

ENTER DATA	ENTER DATA (cont'd)
10.000	-3.113
7.969	-3.138
6.613	-3.320
5.552	-3.530
4.679	-7.816
3.912	-4.556
3.196	-3.721
2.480	-13.352
1.691	-7.566
.653	-5.104
-1.759	-4.410
-1.225	-4.405
-2.170	-4.319
-1.505	-4.499
-2.212	-4.154
-2.033	-4.339
-2.140	-4.357
-2.302	-4.151
-2.549	-4.324
-2.728	-4.250
-2.708	-4.296
-2.790	-4.241
-3.008	-4.382
-2.914	-4.133
-2.982	-4.317

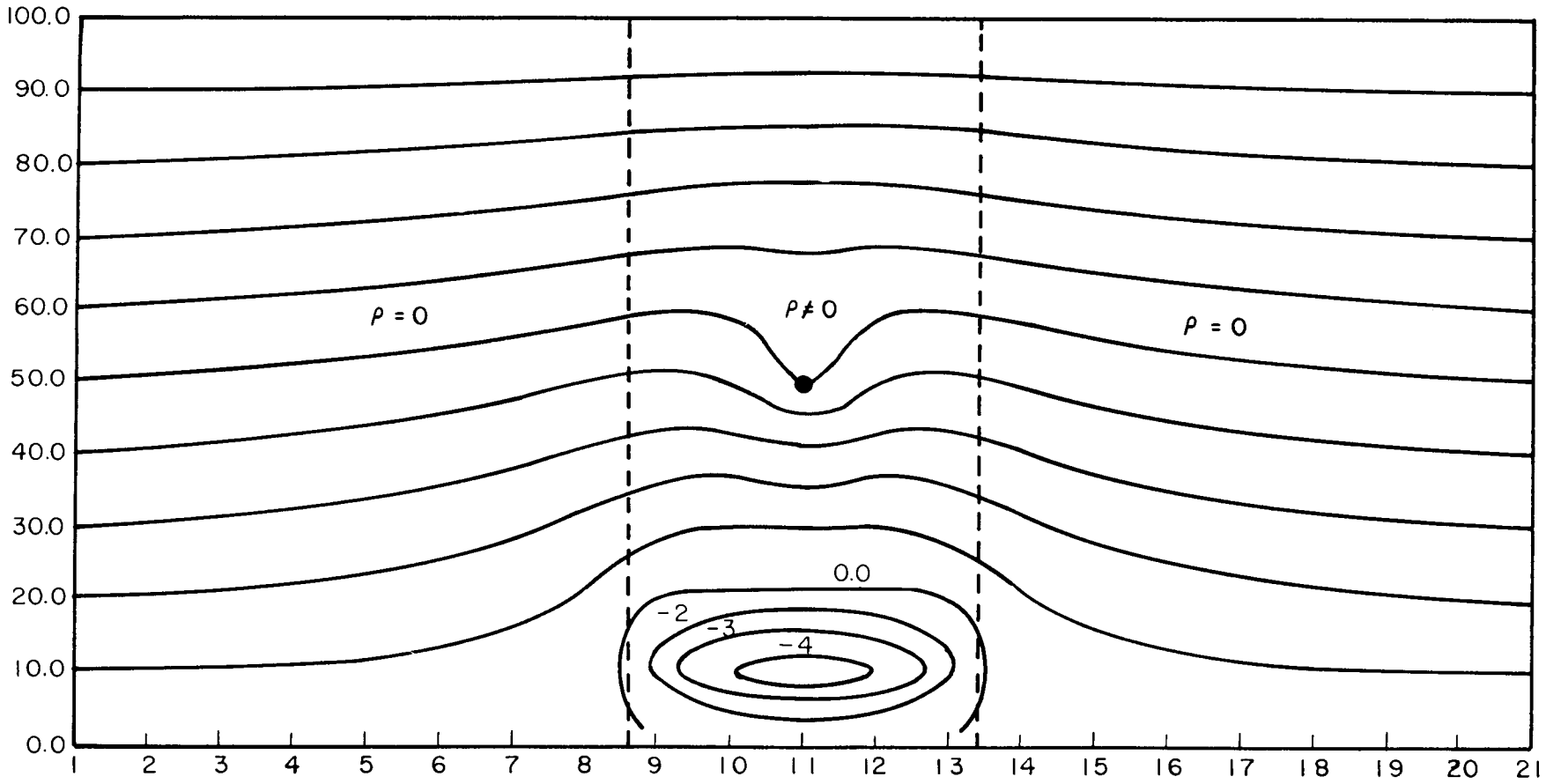

FIG. 12 POTENTIAL FIELD. PROGRAM (III)

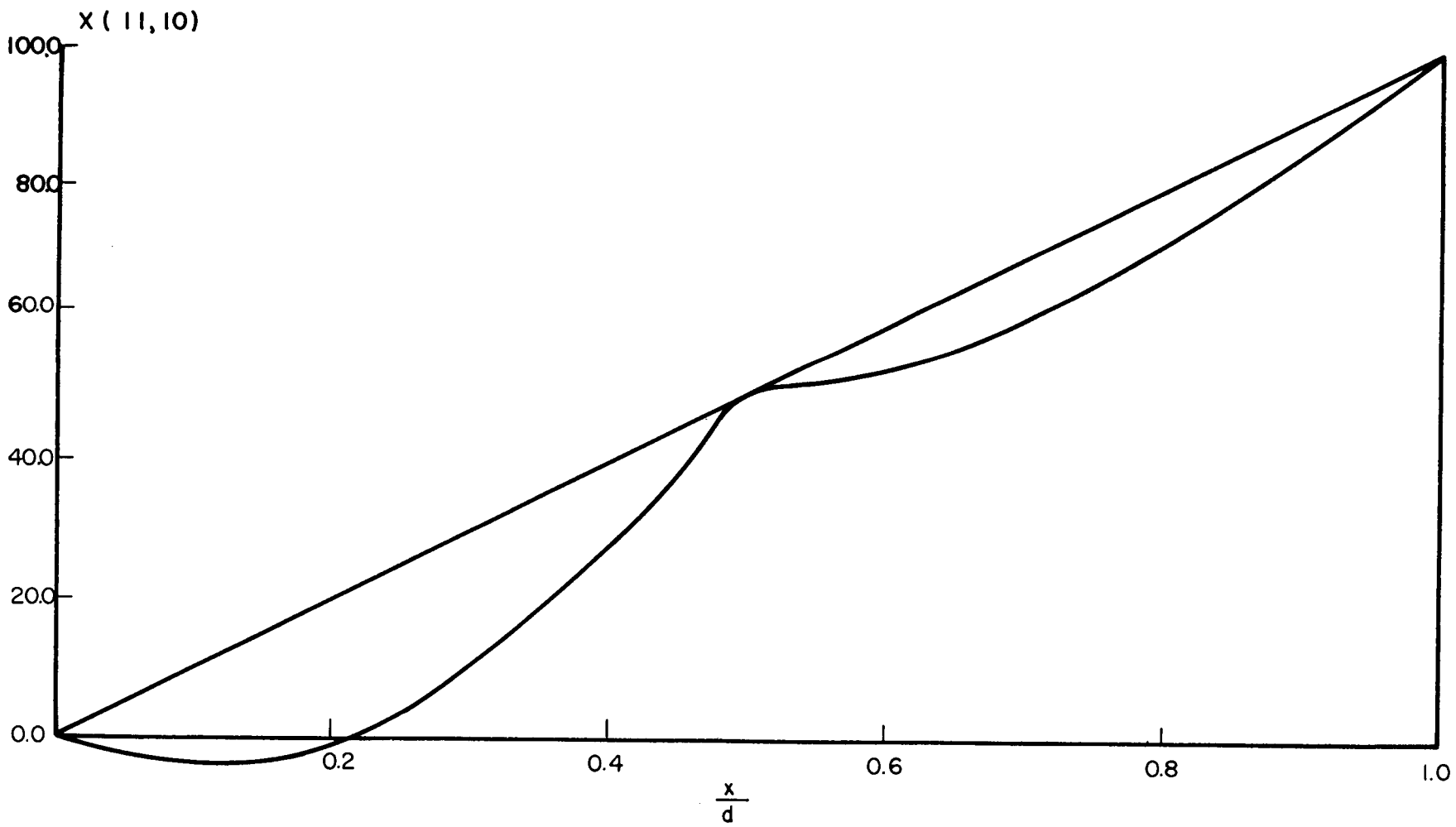

FIG. 13 POTENTIAL DISTRIBUTION PROGRAM (III)